

Article

Axial Behavior of FRP Confined Concrete Using Locally Available Low-Cost Wraps

Asad U. Qazi ¹, Qasim S. Khan ^{1,*}, H. Abrar Ahmad ² and Thong M. Pham ^{3,*}¹ Civil Engineering Department, University of Engineering and Technology, Lahore 54890, Pakistan² Architectural Engineering Department, University of Engineering and Technology, Lahore 54890, Pakistan³ School of Civil and Mechanical Engineering, Curtin University, Bentley 6102, Australia

* Correspondence: qasimkhan@uet.edu.pk (Q.S.K.); thong.pham@curtin.edu.au (T.M.P.)

Abstract: This study investigates the influences of three types of locally available low-cost Fiber Reinforced Polymers (FRP) wraps and two concrete mix designs on the axial behavior of FRP confined concrete. The experimental program comprised four unconfined (control), four glass FRP Matt Strand (GFRP-MS) confined concrete, four glass FRP Rowing (GFRP-R) confined concrete and four carbon FRP (CFRP) confined concrete specimens with a diameter of 150 mm and a height of 300 mm tested under axial compression. The specimens were prepared using two normal strength concrete mix designs, i.e., Mix-A and Mix-B. The experimental results exhibited that an increase in the confined concrete strength per unit cost ratio of a single layer of GFRP-MS was about two times of a single layer of CFRP wrap, whereas the increase in confined concrete strength per unit cost ratio of single layer of GFRP-R was about four times of a single layer of CFRP wrap. GFRP-MS and GFRP-R wraps can exhibit similar confined strengths as CFRP wrap with six and twelve times lower costs, respectively, than CFRP wrap. Mix-B concrete specimens exhibited higher confined concrete strengths but lower confined concrete strain than Mix-A concrete specimens. A database of 140 FRP confined concrete specimens was developed based on a set of specific criteria to develop a design-oriented model to predict the FRP confined concrete strength. The predicted confined concrete strengths matched well with the experimental confined concrete strengths. The two layers of GFRP-R exhibited similar confined concrete strength as CFRP wrap. In addition, GFRP-R exhibited high cement strength index (CSI) and low embodied CO₂ index (CI).

Keywords: FRP confined strength; low-cost; GFRP; CFRP; database; embodied CO₂ index; cement strength index



Citation: Qazi, A.U.; Khan, Q.S.; Ahmad, H.A.; Pham, T.M. Axial Behavior of FRP Confined Concrete Using Locally Available Low-Cost Wraps. *Sustainability* **2022**, *14*, 9989. <https://doi.org/10.3390/su14169989>

Academic Editors: Khoi Nguyen, Md Rajibul Karim and Md Mizanur Rahman

Received: 14 July 2022

Accepted: 10 August 2022

Published: 12 August 2022

Publisher's Note: MDPI stays neutral with regard to jurisdictional claims in published maps and institutional affiliations.



Copyright: © 2022 by the authors. Licensee MDPI, Basel, Switzerland. This article is an open access article distributed under the terms and conditions of the Creative Commons Attribution (CC BY) license (<https://creativecommons.org/licenses/by/4.0/>).

1. Introduction

The construction industry largely depends on the use of concrete, which is a key construction material. Reinforced Concrete (RC) structures are constructed to support the design loads over their design life. However, the load-carrying capacity of RC structures deteriorates over the designed life mainly due to carbonation of concrete and corrosion of steel reinforcement [1,2]. Deteriorated RC structures may require repair and strengthening over the design life. In the last two decades, a large number of RC structures were either repaired or strengthened using different innovative materials and economical techniques [3,4].

The selection of appropriate materials and techniques for repairing and strengthening deteriorated RC structures primarily depends on the availability of materials and financial resources [4,5]. The research investigations are ongoing to seek affordable, strong, and durable materials and develop innovative techniques that can be used to restore the strength of deteriorated RC structural members without significantly increasing the self-weight of structures [6]. In the past, deteriorated RC structural elements were usually strengthened by overlaying a layer of Ordinary Portland Cement (OPC) concrete on the existing deteriorated RC structural elements. However, the overlaying technique resulted in a substantial

increase in the dead load of the structure without significantly increasing its strength [7]. The strengthening of deteriorated columns using RC jacketing significantly enhances the load-carrying capacity of the deteriorated RC columns. However, RC jacketing also results in a large increase in the cross-sectional area of the RC columns and thus increases the self-weight of RC columns. Moreover, the RC jacketing is expensive and requires highly skilled labor [8,9]. Meanwhile, steel jacketing could also be used to strengthen existing deteriorated columns. Steel jacketing is preferred over concrete jacketing, as steel jacketing results in higher confined concrete strengths than concrete jacketing. However, the high cost of steel is a major concern in the wide applications in the construction industry, and it prevents the popular use of steel jacketing. Moreover, steel and concrete have different Poisson's ratios, as such, the two materials undergo lateral expansion at different rates under the applied axial load and generate a gap between steel jacket and confined concrete, which reduces the effectiveness of steel confinement. Moreover, the confinement pressure becomes almost constant when the steel jacket reaches its yield stress [10,11]. In the last three decades, Fiber Reinforced Polymer (FRP) composites have been used as a viable option to strengthen the deteriorated RC beams and columns with a negligible increase in the self-weight of the structural element. FRP sheets significantly increase the strength and ductility of the concrete beams and columns [3,12]. Recently, FRP tube confined concrete beams and columns have been used, respectively, as an alternative to RC beams and columns for new construction. FRP tubes also serve as formworks and longitudinal and transverse reinforcements for the new construction [1,9,13,14].

FRP is considered an excellent material for strengthening because it possesses higher tensile strength, lower self-weight, and higher resistance to corrosion than those made of steel. FRP has found a wide range of applications in civil engineering and is being used in the forms of wraps, tubes, and longitudinal reinforcing bars in concrete members. FRP wraps are the most popular option for enhancing the strength of existing deteriorated RC beams and columns due to its convenience and excellent performance. For the new construction of beams and columns, FRP tubes are often adopted [15–17]. The life-cycle cost of the construction associated with FRP is lower than conventional RC structures, considering the corrosion of steel reinforcement [9,14,18].

In the available literature, numerous research studies investigated the effects of different parameters on the confined concrete strength and confined concrete strain of FRP confined concrete. The different parameters that significantly influence the strength of FRP confined concrete are the type of FRP, concrete properties, fiber properties and orientations of fibers, actual confinement ratio, and confinement methods [4,5,16]. The effectiveness of FRP confinement is directly proportional to the actual confinement ratio and is inversely proportional to the unconfined concrete strength. The confined concrete strength and confined concrete strain increase with the compressive concrete strength. However, the ratio of FRP confined concrete strength (f'_{cc}) to unconfined concrete strength (f'_{co}) decreases with an increase in the unconfined concrete strength [19–23].

The strength enhancement ratio (f'_{cc}/f'_{co}) depends on the fiber type, modulus of elasticity (MOE) of fibers, thickness and rupture strain of the FRP confining materials. Carbon FRP (CFRP) and high modulus CFRP (HMCFRP) confined concretes exhibit a significantly higher increase in the f'_{cc} and confined concrete strain (ductility) than glass FRP (GFRP) and basalt FRP (BFRP) confined concretes, as CFRP and HMCFRP have higher MOE than GFRP and BFRP [18,24]. However, for a lower modulus fiber, i.e., GFRP or BFRP, three to five FRP layers can exhibit a significant increase in the f'_{cc} and ductility [13]. Previous research investigations reported that CFRP confined concrete exhibited a more sudden and brittle failure than GFRP confined concrete, which was attributed to the higher MOE of CFRP than GFRP [24,25]. Moreover, an increase in the slenderness ratio of the confined concrete significantly reduced the f'_{cc} and confined concrete strain [20,26,27]. A limited number of research studies investigated the differences in f'_{cc}/f'_{co} for FRP wrap and FRP tube confinements. Although FRP wraps and FRP tube confined concrete specimens achieved similar stress-strain behavior, FRP wrap confined concrete specimens

exhibited marginally higher confined concrete strength and confined concrete strain than FRP tube confined concrete specimens. This is attributed to the higher bond stress between FRP wrap and confined concrete, as reported in the previous studies [1,14,18,22,23].

Meanwhile, numerous research studies proposed design-oriented stress-strain models of FRP confined concrete to predict the stress-strain behavior of FRP confined concrete, confined concrete strength, and confined concrete strain [28–32]. Earlier, stress-strain models of FRP confined concrete were similar to steel confined concrete [33,34]. In the latter research investigations, bilinear stress-strain models of FRP confined concrete were developed [28,35,36]. In the more recent strength models, the effect of confinement was incorporated on the initial stress-strain curve for FRP confined concrete with higher accuracy than the earlier models [24,30,31,37].

This study focuses on enhancing the axial strengthening of deteriorated normal strength concrete (NSC) specimens using locally available low-cost FRP wraps. This research investigates the axial behavior of NSC specimens strengthened with different types of locally available low-cost FRP wraps. The cost-effectiveness and environmentally friendly benefit of the locally available low-cost GFRP are examined. Moreover, a regression-based model is developed to predict the FRP confined concrete strength with higher accuracy than the existing available models.

2. Materials and Methods

A total of 16 unconfined and FRP confined concrete specimens were prepared using normal strength concrete mix in accordance with ASTM C192/C192M [38] in the Plain and Reinforced Concrete Laboratory, Civil Engineering Department, University of Engineering and Technology, Lahore.

2.1. Materials

In this experimental study, Type I cement was used to prepare concrete. The two normal strength concrete (NSC) mixes with the target slump of 75–80 mm were produced. Two NSC mixes with different mix proportions (cement: sand: coarse aggregate), i.e., Mix-A (1:2:4) and Mix-B (1:1:2), were prepared. The target compressive strengths of Mix-A and Mix-B mixes were 21 MPa and 28 MPa, respectively. Three types of FRP wraps, i.e., high-cost CFRP wrap, locally available low-cost Glass FRP Rowing (GFRP-R) wrap and locally available low-cost Glass FRP Matt Strand (GFRP-MS) wrap, were used. The cost of CFRP wrap was approximately USD 5 per square meter, whereas the costs of locally available GFRP-R and GFRP-MS were USD 0.2 per square meter and USD 0.25 per square meter, respectively, in Fall, 2021 [39]. In CFRP wrapped concrete specimens, Chemdur-300 (epoxy-based resin) was used as a bonding agent as per the requirement of the manufacturer [39]. In the concrete specimens confined with GFRP-R or GFRP-MS, the polyester resin comprising cobalt octate and methyl ethyl ketone peroxide was used as a bonding agent as per the requirement of the manufacturer [39].

The material properties (modulus of elasticity, tensile strength, and rupture strain) of CFRP wrap were provided by the manufacturer, whereas the material properties of GFRP-MS wraps and GFRP-R wraps were determined from the laboratory test results. The GFRP-MS and GFRP-R strips of 250 mm in length and 50 mm in width with aluminum tabs at the ends were prepared according to the ASTM D3039-17 [40] (Figure 1a). The GFRP-MS and GFRP-R strips were tested under displacement-controlled load application at the rate of 1 mm per minute using Keiwei 2000 kN testing machine (Figure 1b). The measured rupture strain of GFRP-MS and GFRP-R were 5.4% and 5.0%, respectively. The measured modulus of elasticity (MOE) and ultimate tensile strength of GFRP-R were two times those of GFRP-MS. The tensile properties of CFRP and tested GFRP-MS and GFRP-R strips are presented in Table 1.

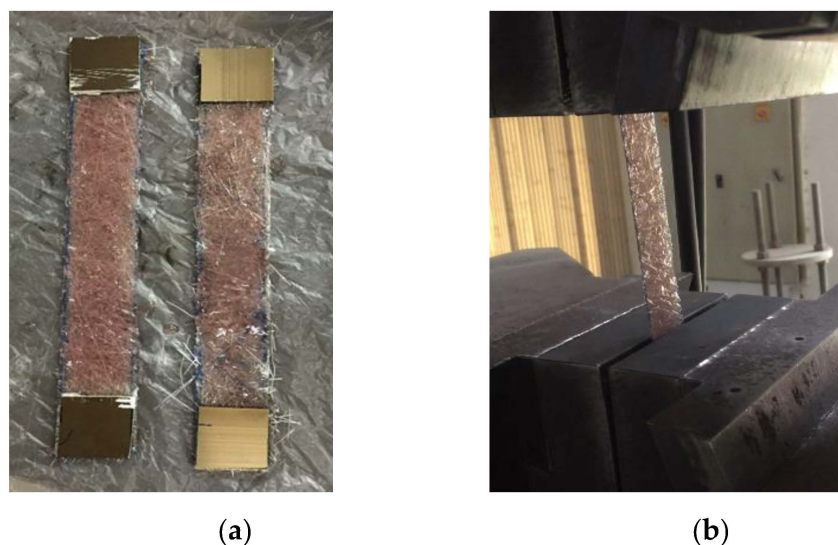


Figure 1. Tensile testing of (a) prepared GFRP strips and (b) placed in the testing machine.

Table 1. Properties of FRP.

FRP Type	Modulus of Elasticity (MPa)	Ultimate Tensile Strength (MPa)	Elongation (%)	Thickness (mm)
GFRP-MS	2480	134	5.4	1.90
GFRP-R	5520	276	5.0	1.75
CFRP	54,000	810	1.5	1.40

2.2. Specimen Preparation and Testing

A total of 16 NSC specimens of 150 mm diameter and 300 mm height were cast in two groups. In the first group, eight NSC specimens were prepared using Mix-A. In the second group, another eight NSC specimens were prepared using Mix-B. Each group comprises two unconfined NSC (control) specimens, two GFRP-MS wrapped NSC specimens, two GFRP-R wrapped NSC specimens, and two CFRP wrapped NSC specimens (Table 2). Two identical NSC specimens were cast to ensure the reliability of the test. All the NSC specimens were cast in steel molds of 150 mm in diameter and 300 mm in height (Figure 2). All the tested specimens were cured at room temperature of 23 ± 2 °C with a relative humidity of about 90% for 28 days [38]. Afterwards, the test specimens except the control specimens were wrapped with a single layer of FRP with an overlap of 100 mm.

Table 2. Details of the tested specimens.

Mix/ Concrete Mix Proportion	No. of Specimens			
	Control Specimen (Unconfined)	GFRP-MS Confined	GFRP-R Confined	CFRP Confined
A	2	2	2	2
B	2	2	2	2



Figure 2. Casting of concrete specimens.

The test specimens were instrumented with Linear Variable Displacement Transducers (LVDTs). In addition, strain gauges were attached on FRP confined NSC specimens at the mid-height of the specimen, each in the axial and hoop directions. The specimens were tested at the loading rate of 0.5 mm/min using a Shimadzu 1000 kN Universal Testing Machine (UTM) in accordance with ASTM C39-18 [41] (Figure 3).

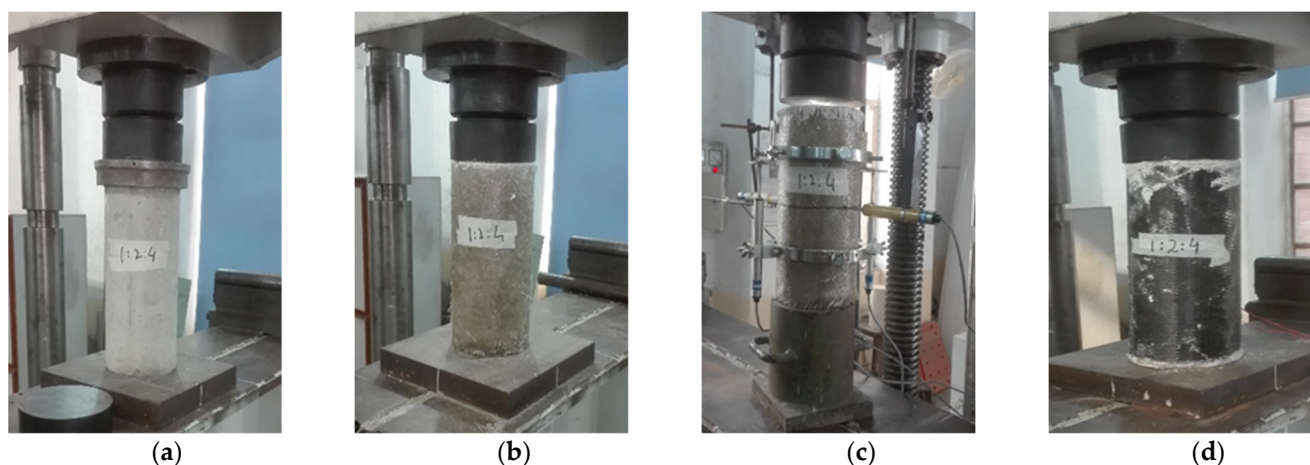


Figure 3. Concrete test specimens: (a) Unconfined, (b) GFRP-MS confined, (c) GFRP-R confined, and (d) CFRP confined.

3. Results

3.1. Observed Failure Pattern

The unconfined NSC (control) specimens of Mix-A and Mix-B failed due to the crushing of concrete. The GFRP-MS, GFRP-R, and CFRP confined NSC specimens failed due to the brittle rupture of FRP wrap along with the crushing of concrete. In locally available low-cost GFRP-MS and GFRP-R confined NSC specimens, the failure was initiated at the mid-height of the specimen due to the splitting of fibers in the vertical direction. The final failure was due to the rupture of the FRP wrap with the minimal crushing of concrete. In CFRP confined NSC specimens, the failure was initiated with a snapping sound of splitting of fibers at the mid-height of the specimen in the hoop direction. The final failure was due to the rupturing of the fibers and crushing of concrete (Figure 4).

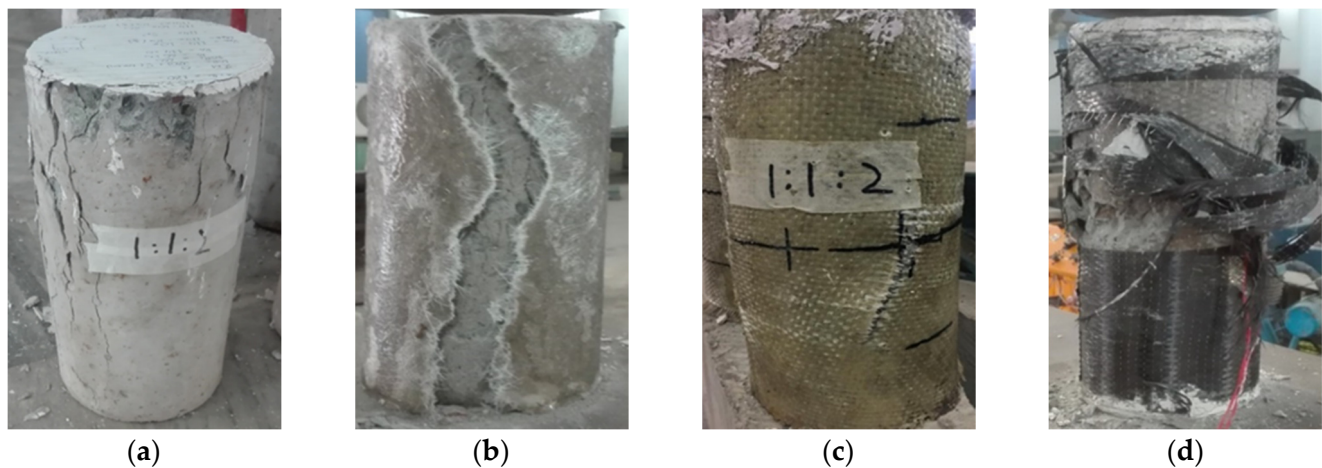


Figure 4. Failure modes: (a) Unconfined, (b) GFRP-MS confined, (c) GFRP-R confined, and (d) CFRP confined concrete specimens.

3.2. Experimental Results of Unconfined and FRP Confined Concrete Specimens

The experimental results of the tested specimen are presented in Table 3. The influences of types of FRP wrap and NSC mix proportions on the peak confined concrete stress and axial and lateral strain at peak axial stress are presented in Table 4 and are discussed in the following sections.

Table 3. Compressive strengths of test specimens.

Mix ID.	Unconfined Concrete Strength f'_{co} (MPa)	GFRP-MS Confined Concrete Strength f'_{cc} (MPa)	Strength Enhancement Ratio	GFRP-R Confined Concrete Strength f'_{cc} (MPa)	Strength Enhancement Ratio	CFRP Confined Concrete Strength f'_{cc} (MPa)	Strength Enhancement Ratio
Mix A	24.3	26.3	1.08	28.2	1.16	44.1	1.81
Mix B	29.3	32.0	1.09	34.4	1.17	50.2	1.71

Table 4. Peak axial stress, axial strain, and lateral strain at peak axial stress of FRP confined concrete.

Mix ID	Confinement Type	Peak Confined Concrete Stress (MPa)	Axial Strain at Peak Axial Stress (%)	Lateral Strain at Peak Axial Stress (%)
Mix A	GFRP-MS	26.3	0.19	0.23
Mix B		32.0	0.21	0.25
Mix A	GFRP-R	28.2	0.43	0.33
Mix B		34.4	0.19	0.29
Mix A	CFRP	44.1	0.61	0.64
Mix B		50.2	0.45	0.71

3.2.1. Influence of Type of FRP Wraps

The FRP wrap type exhibited a significant influence on the FRP confined concrete strength. The CFRP confined concrete specimens exhibited the highest strength enhancement ratio (f'_{cc}/f'_{co}), whereas GFRP-MS exhibited the lowest f'_{cc}/f'_{co} . The GFRP-MS confined concrete specimens showed f'_{cc}/f'_{co} of 1.08 and 1.09, respectively, for NSC Mixes A and B (Table 3). The GFRP-R confined concrete specimens showed f'_{cc}/f'_{co} of 1.16 and 1.17, respectively, for concrete Mixes A and B (Table 3). The CFRP confined concrete specimens showed f'_{cc}/f'_{co} of 1.81 and 1.71, respectively, for NSC Mixes A and B (Table 3). As can be seen that GFRP-MS and GFRP-R confined concrete specimens exhibited lower f'_{cc} than CFRP confined concrete specimens. Although GFRP-MS and GFRP-R confined

concrete exhibited lower f'_{cc}/f'_{co} , they were effective in confining the dilated concrete (Figure 5).

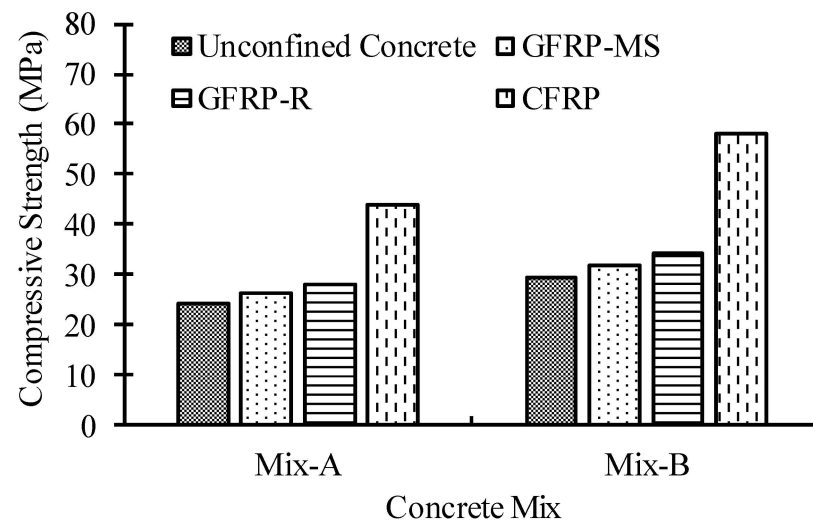


Figure 5. Influence of FRP type confinement on confined concrete strength.

The FRP confinement is mainly dependent on the elastic modulus and tensile strength of FRP confining material. The CFRP confined concrete specimens achieved an average (Average of Mix A and Mix B) of 1.62 and 1.51 times higher confined concrete strengths, respectively, than GFRP-MS confined concrete and GFRP-R confined concrete specimens. The CFRP confined concrete specimens achieved an average of 2.68 and 1.50 times higher confined concrete strain at peak axial stresses, respectively, than GFRP-MS confined concrete and GFRP-R confined concrete specimens. The CFRP confined concrete specimens exhibited an average of 2.81 and 2.19 times higher lateral strain at peak axial stresses, respectively, than GFRP-MS confined concrete and GFRP-R confined concrete specimens (Table 4). The higher average confined concrete strengths and strain of CFRP confined concrete specimens are attributed to higher modulus of elasticity, ultimate tensile strength, and rupture strain of CFRP wrap, which resulted in higher confinement pressures and consequently produced higher confined concrete stresses and strain. On the other hand, the locally available low-cost GFRP wraps exhibited comparatively low average tensile strengths and rupture strain. Hence, GFRP-MS and GFRP-R confined specimens exhibited a lower increase in the confined concrete strengths and strain. The GFRP-R showed an average of 1.07 times higher confined concrete strength and an average of 1.55 times higher confined concrete strain at peak axial stress than GFRP-MS confined concrete specimens. This is attributed to the fact that the modulus of elasticity and ultimate tensile strength of GFRP-R were almost two times those of GFRP-MS.

In addition, CFRP wrap is about twenty times more expensive than low-cost GFRP-MS, and CFRP wrap is about twenty-five times more expensive than low-cost GFRP-R wraps. GFRP-MS wrap is about 1.25 times more expensive than GFRP-R wrap. The increase in the confined concrete strength per unit cost ratio of single layers of GFRP-R, GFRP-MS, and CFRP wraps were 1.17, 1.08, and 1.04, respectively. The increase in the confined concrete strength per unit cost ratio of a single layer of GFRP-R is about four times of CFRP wrap, whereas the increase in confined concrete strength per unit cost ratio of a single layer of GFRP-MS is about two times of CFRP wrap. The increase in the confined concrete strength per unit cost ratio of GFRP-R is about two times of GFRP-MS. Hence, locally available GFRP-MS and GFRP-R confining materials are viable options to strengthen the existing concrete specimens when the strength enhancement requirement is not very high. Moreover, the GFRP-MS and GFRP-R are easily locally available and economical, whereas CFRP is an expensive option.

3.2.2. Influence of Different Concrete Mix Proportions

The peak axial stress (confined concrete strength) and the corresponding axial and lateral strain at peak axial stresses of all three types of FRP confined concrete specimens varied with the concrete mix proportions. The unconfined NSC strengths of Mix-A and Mix-B were 24.3 MPa, and 29.3 MPa, respectively. It is noted that the target unconfined NSC strengths of Mix A and Mix B were 21 MPa and 28 MPa, respectively. Generally, the 21 MPa unconfined NSC strength is commonly used in the construction of flexural members, whereas 28 MPa unconfined NSC strength is often adopted for the construction of axial members in Pakistan. The unconfined NSC strengths of Mix-A and Mix-B were higher than the target concrete strengths because of the relatively low water to cement ratio used in the preparation of these concrete mixes. The FRP confined concrete strengths of NSC specimens prepared using Mix B were about 19.3% higher than that of NSC specimens prepared using Mix A (Figure 6). The confined concrete strain at peak axial stress of FRP confined concrete specimens prepared with Mix B was about 24% lower than concrete specimens prepared with Mix A. (Table 4). Mix A contained 14.3% cement, while 25% cement was used in Mix B. The higher cement content resulted in higher unconfined concrete strengths due to the increased cement hydration process and consequently resulted in higher confined concrete strengths. Meanwhile, the higher quantities of cement in the concrete mix proportion resulted in increased brittleness and consequently lower confined concrete strain of FRP confined concrete.

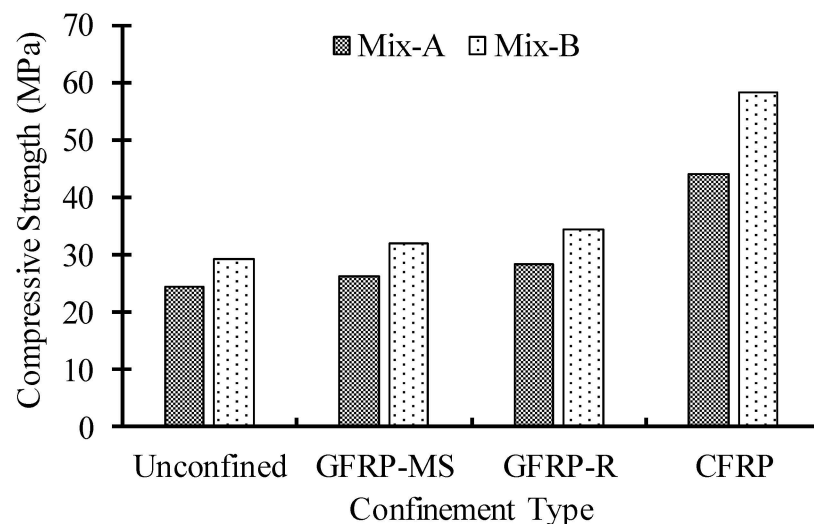


Figure 6. Influence of concrete types on confined concrete strengths.

3.3. Axial Stress versus Strain Curves of FRP Confined Concrete

Axial stress-axial strain ($\sigma - \varepsilon$) and axial stress - lateral strain ($\sigma - \varepsilon_l$) curves of GFRP-MS confined concrete specimens, GFRP-R confined concrete specimens, and CFRP confined concrete specimens are presented in Figure 7. The $\sigma - \varepsilon$ and $\sigma - \varepsilon_l$ curves of CFRP confined concrete specimens initially exhibited similar behavior to that of conventional unconfined concrete, as CFRP confinement was inactive at low load levels. However, the ascending second branch of $\sigma - \varepsilon$ and $\sigma - \varepsilon_l$ curves of all the CFRP confined concrete specimens indicated the activation of CFRP confinement in confining the dilated concrete. In the case of GFRP-MS confined concrete specimens and GFRP-R confined concrete specimens, the first branches of $\sigma - \varepsilon$ and $\sigma - \varepsilon_l$ curves were similar to those of conventional unconfined concrete. However, GFRP-R and GFRP-MS did not exhibit the steep ascending second branches of the $\sigma - \varepsilon$ and $\sigma - \varepsilon_l$ curves, which indicated that confinement pressure exerted by GFRP-MS and GFRP-R wraps on dilating concrete was lower than that of CFRP confined concrete. This is attributed to the significantly lower modulus of elasticity, and ultimate tensile strengths of GFRP-MS and GFRP-R wraps, which resulted in lower confinement

pressures applied on the dilating concrete and subsequently resulted in a lower increase in the confined concrete strengths. However, with a significantly lower cost, about four layers of GFRP-MS and two layers of GFRP-R can be used to achieve an equivalent performance to one layer of CFRP confined concrete. This estimation can be confirmed by using the proposed empirical model below.

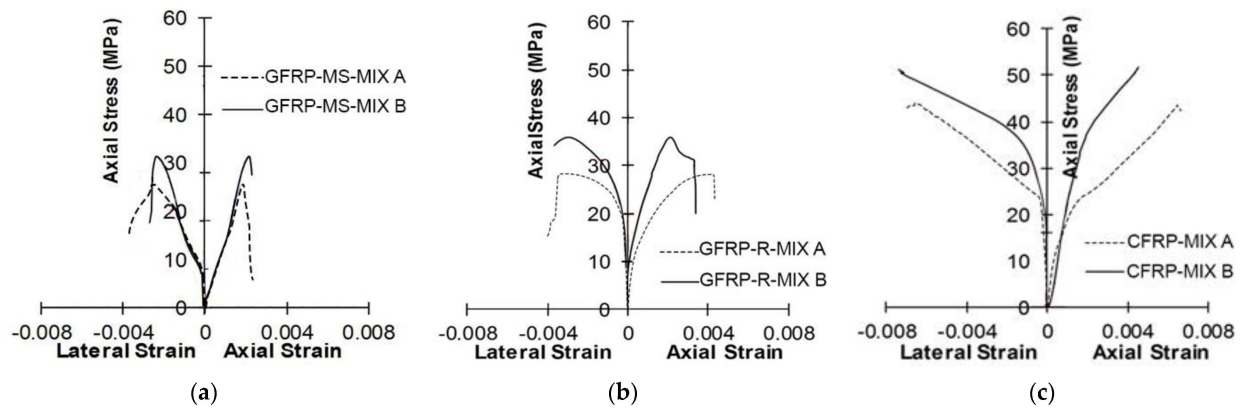


Figure 7. Axial stress-strain curves of (a) GFRP-MS confined concrete, (b) GFRP-R confined concrete, and (c) CFRP confined concrete specimens.

4. Analytical Approach

In this section, a database of FRP confined concrete specimens tested in the axial compression is established to develop a strength enhancement ratio model for the prediction of FRP confined concrete strengths. In addition, experimental CFRP, GFRP-R, and GFRP-MS confined concrete strengths are compared with analytical FRP confined concrete strengths predicted with the developed strength enhancement ratio model. In the available research studies, the strength enhancement ratio models of FRP confined concrete are given in the form of Equation (1) which was initially proposed by Richart et al. [42].

$$\frac{f'_{cc}}{f'_{co}} = 1 + k_1 \left(\frac{f_l}{f'_{co}} \right) \quad (1)$$

where f'_{cc} is the confined concrete strength, f'_{co} is unconfined compressive concrete strength, f_l is lateral confining pressure, and k_1 is strength enhancement coefficient. Richart et al. [42] proposed Equation (1) for actively confined concrete with $k_1 = 4.1$. Fardis and Khalili [32] modified Richart et al. [42] model for FRP confined concrete by redefining the f_l in Equation (1), as follows:

$$f_l = \frac{2f_{FRP}t}{D} \quad (2)$$

where f_{FRP} is the tensile rupture strength of the FRP, t is the thickness, and D is the diameter of circular specimens.

In the available literature, various research studies compiled databases of FRP confined concrete, as summarized in Table 5. These research studies proposed design models similar to Equation (1) using regression analysis. It is pertinent to mention that the confinement provided by FRP increases linearly until rupture, unlike steel confinement, which starts yielding after a certain magnitude of confinement pressure, as reported in Fardis and Khalili [32] and Richart et al. [42].

Table 5. Summary of FRP wrap database.

References	D (mm)	H (mm)	f'_{co} (MPa)	f'_{co}/f'_{cc}	k_1
Lea et al. [43]	200	400	18.91	1.09	2.3
Vincent and Ozbakkaloglu [44]	152	305	44.8	1.61–1.67	2.05
Tara and Ashim [45]	103	200	20	0.67–1.08	2.3
Vincent and Ozbakkaloglu [22]	152	305	35.5	1.24	2.06
Ozbakkaloglu and Lim [17]	100	200	49.4	1.23	2.15
Jalal and Ramezani pour [46]	132	294	17.4–39.7	1.8–1.95	2.1–2.3
Akogbe et al. [47]	100	200	25.2–28.1	2.36–2.55	2.21–2.25
Dai et al. [48]	152	305	32.5–39.2	1.19–1.6	2.17–4.19
Aire et al. [23]	150	300	42	0.97–1.1	2.05
Cui and Sheikh [19]	150	300	45.7–48.1	1.23–1.8	1.5–3.58
Eid et al. [49]	152	300	32.1–48	1.04–1.09	3.6–3.9
Almusallam [50]	150	300	47.7–50.8	1.0–1.18	2.66–2.99
Valdmanis et al. [51]	150	300	20–40	1.64–2.4	3.54–3.93
Wu and Wang [52]	150	300	31.2–32.3	1.01–1.4	3.7–3.8
Jiang and Teng [37]	152	305	44.2–45.9	1.0–1.4	3.01–3.03
Picher F. [53]	152	305	39.7	1.41	2.3
Tamuzs et al. [54]	150	300	20.5–51.8	1.2–1.4	3.44–3.93
Lam et al. [55]	152	305	41.1	1.27	3.3
Campione G. [56]	100	200	20	2.47	4.08
Matthys et al. [36]	150	300	34.9	1.3	2.32
Lam and Teng [57]	152	305	35.9	1.4	3.3
Theriault et al. [58]	51	102	37	1.7–1.89	3.77
Harries and Carey [59]	152	305	32.1	1.03–1.15	3.45–3.90
Ibrahim et al. [60]	150	300	25.6–29.8	1.7–1.9	4.12
Rousakis and Tepfers [61]	152	305	25.8–49.1	1.49–1.61	4.09
Shahawy et al. [62]	152.5	305	19.4–49	1.21–1.74	3.6–4.02
Xiao and Wu [63]	152	305	33.7–55	1.05–1.45	4.13
Owen L. [35]	152	305	47.5	1.37	2.66
Owen L. [35]	102	203	53	1.33	2.8
Karbhari and Gao [64]	152	305	38.38	1.16	2.33
Howie and Karbhari [34]	152.4	304.8	42.49	1.05	2.38

4.1. FRP Wrap Database

In this study, an extensive review of available existing FRP confined concrete studies has been conducted to compile a database of FRP confined concrete specimens (Table 5). The database was established by defining a set of limiting criteria to develop a reliable and consistent database of FRP confined concrete to predict the strength enhancement ratio coefficient and hence the FRP confined concrete strength (Table 6). The following limiting criteria were considered for the establishment of the database:

- i. The database was limited to the FRP wrapped specimens. The FRP tube specimens were excluded.
- ii. The database comprises FRP confined concrete specimens with concrete compressive strengths between 17 and 55 MPa (normal strength concrete). High strength and ultra-high strength FRP confined concrete specimens were not considered in this database.
- iii. The database comprises specimens with a height to diameter ratio of up to three. The specimens with a height to diameter greater than three were excluded from the database.
- iv. The database included only specimens of circular cross-sections. Specimens of rectangular and square cross-sections were excluded from the database.
- v. The concrete specimens confined with the continuous FRP wrap were included. Specimens confined with intermittent FRP wraps were not considered in the database.
- vi. Only externally FRP confined concrete specimens were included in the database. Specimens reinforced with longitudinal and transverse steel and FRP reinforcements were excluded from the database.
- vii. The datasets from existing studies with incomplete material and physical properties were not included in the database.

Table 6. Database for strength enhancement coefficient.

References	D (mm)	H (mm)	f_{co} (MPa)	f'_{co}/f'_{cc}	k_1
Lea et al. [43]	200	400	18.91	1.09	2.31
	200	400	18.91	1.09	2.31
	200	400	18.91	1.09	2.31
Tara and Ashim [45]	103	200	20	1.08	2.3
	103	200	20	0.93	2.3
	103	200	20	0.87	2.3
	103	200	20	0.67	2.3
	152	305	35.5	1.24	2.15
Ozbakkaloglu and Lim [17]	152	305	35.5	1.24	2.15
	152	305	35.5	1.21	2.15
	152	305	44.8	1.61	2.05
	152	305	44.8	1.67	2.05
	100	200	49.4	2.21	2.06
Vincent and Ozbakkaloglu [22,44]	100	200	49.4	2.09	2.06
	100	200	49.4	2.13	2.06
	100	200	49.4	2.18	2.06
	100	200	49.4	2.10	2.06
	100	200	49.4	2.23	2.06
	132	294	39.68	1.95	2.1
Jalal and Ramezani-pour [46]	132	294	17.39	1.80	2.3
	100	200	25.2	2.55	2.25
Akogbe et al. [47]	100	200	25.9	2.43	2.25
	100	200	28.1	2.36	2.21
	100	200	26.8	2.42	2.23
	152	305	39.2	1.57	4.19
	152	305	39.2	1.60	4.19
	152	305	39.2	1.42	4.19
	152	305	39.2	1.40	4.19
	152	305	39.2	1.34	4.19
Dai et al. [48]	152	305	39.2	1.29	4.19
	152	305	39.2	1.20	4.19
	152	305	39.2	1.36	4.19
	152	305	39.2	1.11	2.17
	152	305	32.5	1.28	2.17
	152	305	32.5	1.28	2.17
	152	305	32.5	1.30	2.17
	152	305	32.5	1.30	2.17
Aire et al. [23]	150	300	42	0.98	2.05
	150	300	42	1.10	2.05
	150	300	42	0.98	2.05
	150	300	48.1	1.68	2.95
	150	300	48.1	1.80	3.46
	150	300	48.1	1.75	3.25
	150	300	48.1	1.83	3.58
	150	300	47.76	1.24	1.5
	150	300	47.76	1.25	1.59
	150	300	47.76	1.33	2.69
Cui and Sheikh [19]	150	300	47.76	1.31	2.03
	150	300	45.6	1.27	2.28
	150	300	45.6	1.21	1.85
	150	300	45.6	1.23	2.02
	150	300	45.6	1.29	2.48
	150	300	45.7	1.48	3.07
	150	300	45.7	1.40	2.59
	150	300	45.7	1.44	2.84
	150	300	45.7	1.44	2.85

Table 6. Cont.

References	D (mm)	H (mm)	f_{co} (MPa)	f_{co}/f_{cc}	k_1
Eid et al. [49]	152	300	32.1	1.10	3.69
	152	300	32.1	1.10	3.69
	152	300	32.1	1.10	3.69
	152	300	48	1.04	3.92
	152	300	48	1.04	3.92
	152	300	48	1.04	3.92
	150	300	47.7	1.19	2.66
Almusallam [50]	150	300	47.7	1.19	2.66
	150	300	50.8	1.09	2.99
	150	300	50.8	1.09	2.99
	150	300	50.8	1.09	2.99
	150	300	20	2.06	3.54
Valdmanis et al. [51]	150	300	20	2.43	3.54
	150	300	40	1.65	3.93
	150	300	40	1.64	3.93
	150	300	31.4	1.02	3.79
Wu and Wang [52]	150	300	31.2	1.03	3.79
	150	300	32.3	1.01	3.81
	150	300	31.7	1.02	3.8
Jiang and Teng [37]	152	305	45.9	1.05	3.03
	152	305	45.9	1.00	3.03
	152	305	45.9	1.20	3.03
	152	305	44.2	1.09	3.01
	152	305	44.2	1.42	3.01
Picher F. [53]	152	305	39.7	1.41	2.3
	152	305	39.7	1.40	2.3
	152	305	39.7	1.41	2.3
	150	300	25.2	1.40	3.55
Tamuzs et al. [54]	150	300	47.4	1.37	3.9
	150	300	51.8	1.20	3.95
	150	300	20.5	1.40	3.44
	150	300	40.7	1.35	3.81
	150	300	44.3	1.28	3.86
Lam et al. [55]	150	300	49.7	1.40	3.93
	152	305	41.1	1.28	3.3
	152	305	41.1	1.28	3.3
Campione G. [56]	152	305	41.1	1.28	3.3
	100	200	20.05	2.47	4.08
	100	200	20.00	2.45	4.08
Matthys et al. [36]	100	200	20.05	2.47	4.08
	150	300	34.9	1.32	2.32
Lam and Teng [57]	150	300	34.9	1.31	2.32
	150	300	34.9	1.31	2.32
	152	305	35.9	1.40	3.3
Theriault et al. [58]	152	305	35.9	1.40	3.3
	152	305	35.9	1.40	3.3
	51	102	37	1.89	3.77
	51	102	37	1.89	3.77
	51	102	37	1.89	3.77
	51	102	37	1.73	3.77
Harries and Carey [59]	51	102	37	1.73	3.77
	51	102	37	1.73	3.77
	152	305	32.1	1.03	3.45
	152	305	32.1	1.15	3.9
Ibrahim et al. [60]	152	305	32.1	1.10	3.7
	150	300	25.6	1.71	4.12
	150	300	29.8	1.91	4.12
	150	300	29.0	1.80	4.12

Table 6. Cont.

References	D (mm)	H (mm)	f'_{co} (MPa)	f'_{co}/f'_{cc}	k_1
Rousakis and Tepfer [61]	152	305	25.8	1.61	4.09
	152	305	25.8	1.50	4.09
	152	305	49.1	1.60	4.09
	152	305	48.8	1.49	4.09
	152.5	305	19.4	1.74	3.6
	152.5	305	19.4	1.74	3.6
	152.5	305	19.4	1.74	3.6
Shahawy et al. [62]	152.5	305	19.4	1.74	3.6
	152.5	305	49	1.21	4.02
	152.5	305	49	1.21	4.02
	152.5	305	49	1.21	4.02
	152.5	305	49	1.21	4.02
	152.5	305	49	1.21	4.02
	152.5	305	49	1.21	4.02
Xiao and Wu [63]	152	305	33.7	1.05	4.13
	152	305	33.7	1.05	4.13
	152	305	33.7	1.05	4.13
	152	305	55.2	2.83	4.13
	152	305	55.2	2.83	4.13
	152	305	55.2	2.83	4.13
	152	305	33.7	1.45	4.13
	152	305	33.7	1.45	4.13
	152	305	33.7	1.45	4.13
	152	305	43.8	1.10	4.13
Owen L. [35]	152	305	47.5	1.38	2.66
	102	203	53	1.33	2.8
Karbari and Gao [64]	152	305	38.38	1.17	2.33
Howie and Karbhari [34]	152.4	304.8	42.49	1.06	2.38

4.2. Development of Strength Enhancement Coefficient

The strength enhancement coefficient (k_1) was developed based on the regression analysis of the compiled database of 140 data sets (Table 6). A linear regression relationship between strength enhancement coefficient (k_1) and unconfined concrete strengths (f'_{co}) was developed (Equation (3)).

$$k_1 = 3.23 - 0.001f'_{co} \quad (3)$$

Equation (3) was used to calculate the k_1 for the given 140 data sets of the compiled databases. The k_1 was computed to be 3.2 and the computed k_1 was used in Equation (1). Consequently, the following linear equation (Equation (4)) is proposed to predict the FRP confined concrete strengths.

$$f'_{cc} = f'_{co} + 3.2f_l \quad (4)$$

4.2.1. Comparison of Experimental and Computed FRP Confined Concrete Strength

A comparison of the experimental CFRP, GFRP-MS, and GFRP-R confined concrete strengths was carried out with f'_{cc} computed using the developed regression model (Equation (4)). The computed f'_{cc} of CFRP, GFRP-R, and GFRP-MS matched well with the corresponding experimental f'_{cc} . The developed regression model underestimated the f'_{cc} of GFRP-R and GFRP-MS by 14.5% and 5%, respectively. The experimental and computed f'_{cc} of CFRP confined concrete specimens were similar (1%).

4.2.2. Comparison of Experimental Confined Concrete Strengths with Existing Models

A comparison of percentage differences in experimental f'_{cc} and computed f'_{cc} using well-known existing regression models is presented in Table 7. Lam and Teng [27] overestimated the CFRP f'_{cc} by 2% and underestimated the GFRP-R and GFRP-MS f'_{cc} by 13.7% and 5.7%, respectively. Wu and Zhou [65] underestimated the CFRP, GFRP-R, and GFRP-MS f'_{cc} by 16.3%, 14.0% and 5.7%, respectively. Pham and Hadi [26] overestimated the CFRP f'_{cc} by 7.7% and underestimated the GFRP-R and GFRP-MS f'_{cc} by 3.7% and 11%, respectively. Pour et al. [66] overestimated the CFRP f'_{cc} by 12.67% and underestimated the GFRP-R and GFRP-MS by 13.33% and 5.7%, respectively.

Table 7. Comparison between experimental and analytical results.

Confinement Type	Concrete Mix ID	Percentage Differences between Experimental and Analytical Compressive Strength of FRP-Confined Concrete (%)			
		Lam and Teng [27]	Wu and Zhou [65]	Pham and Hadi [26]	Pour et al. [66]
CFRP	Mix A	−3	16	6	12
	Mix B	−1	16	10	13
GFRP-MS	Mix A	1	1	−14	2
	Mix B	9	8	−4	9
GFRP-R	Mix A	11	12	−9	12
	Mix B	17	17	5	14

The comparisons of experimental f'_{cc} with a developed regression model (Equation (4)) and experimental f'_{cc} with well-known existing models exhibited that the developed regression model (Equation (4)) predicted the f'_{cc} of CFRP, GFRP-R, and GFRP-MS specimens with higher accuracy than the existing models.

4.2.3. Cost-Effectiveness of GFRP-R and GFRP-MS

The above model was adopted to predict the confined strengths of GFRP-MS confined concrete, GFRP-R confined concrete and compared to that of CFRP confined concrete. Accordingly, one layer of CFRP confined concrete yielded the confined concrete strengths of 44.1 MPa and 50.2 MPa for Mix A and Mix B, respectively. If GFRP-R and GFRP-MS were used, about two layers and four layers were respectively required to generate equivalent confining pressures and confined concrete strengths as of one layer of CFRP confined concrete. The cost of CFRP is USD 5 per square meter, while the cost of GFRP-R and GFRP-MS is USD 0.20 per square meter and USD 0.25 per square meter, respectively. As a result, to increase the concrete strength from 24.3 MPa (unconfined concrete) to 44.1 MPa, USD 0.86 (86 cents) is required for CFRP, while the costs of GFRP-R and GFRP-MS are USD 0.07 (7 cents) and USD 0.15 (15 cents), respectively. The two layers of GFRP-R can give similar confined concrete strength as one layer of CFRP with almost 12 times lower cost. Similarly, the four layers of GFRP-MS can give similar confined concrete strength as one layer of CFRP with almost 6 times lower cost. This observation suggests that the use of low-cost locally available GFRP-R is a viable option for wide use in the construction industry.

4.2.4. Environmental Assessment

The environmental impact of unconfined, GFRP-MS confined, GFRP-R confined, CFRP confined concrete specimens are assessed based on carbon dioxide (CO₂) emissions in terms of embodied carbon dioxide (e-CO₂) emissions. The e-CO₂ emissions of OPC, coarse and fine aggregates, CFRP and GFRP wraps, and water were obtained from the available research studies to evaluate the eco-friendly performance of FRP confined concrete specimens compared with unconfined concrete specimens. The considered e-CO₂ emissions of OPC is 0.8300 kg/kg, natural aggregates is 0.0459 kg/kg, sand is 0.0139 kg/kg and water is 0.0003 kg/kg [67]. The considered e-CO₂ emissions of CFRP fibers is 42.1410 kg/kg, epoxy is 13.1690 kg/kg, GFRP fibers is 5.2676 kg/kg and polyester resin is 14.8085 kg/kg [68,69]. The computed e-CO₂ emissions of CFRP wraps based on 65% CFRP fibers, and 35% epoxy is 32.0008 kg/kg. The computed e-CO₂ emissions of GFRP wraps based on 70% GFRP

fibers and 30% polyester resin is 8.1300 kg/kg. The eight cylinders of Mix-A comprised a total of 14.54 kg of cement, 29.09 kg of sand, 58.17 kg of coarse/natural aggregates, and 8 kg of water. The eight cylinders of Mix-B comprised a total of 18.51 kg of cement, 27.77 kg of sand, 55.53 kg of coarse/natural aggregates and 9.25 kg of water.

The computed e-CO₂ emissions of Mix-A, unconfined NSC (control) is 1.8931 kg, GFRP-MS confined concrete is 3.5191 kg, GFRP-R confined concrete is 3.2752 kg and CFRP confined concrete is 6.6943 kg. The computed e-CO₂ emissions of Mix-B, unconfined NSC (control) is 2.2873 kg, GFRP-MS confined concrete is 3.9133 kg, GFRP-R confined concrete is 3.6694 kg, and CFRP confined concrete is 7.0874 kg.

The embodied CO₂ index (CI) is calculated as a ratio of e-CO₂ to concrete strength. The CI of Mix-A of control NSC is 0.078 kg/MPa, GFRP-MS confined concrete is 0.134 kg/MPa, GFRP-R confined concrete is 0.116 kg/MPa and CFRP confined concrete is 0.152 kg/MPa. The CI of Mix-B of control NSC is 0.078 kg/MPa, GFRP-MS confined concrete is 0.122 kg/MPa, GFRP-R confined concrete is 0.107 kg/MPa and CFRP confined concrete is 0.141 kg/MPa.

The cement strength contribution index (CSI) is calculated as a ratio of concrete strength (unconfined or confined) to cement content. The CSI of Mix-A of control NSC is 0.071 MPa/kg, GFRP-MS confined concrete is 0.077 MPa/kg, GFRP-R confined concrete is 0.082 MPa/kg and CFRP confined concrete is 0.129 MPa/kg. The CSI of Mix-B of control NSC is 0.067 MPa/kg, GFRP-MS confined concrete is 0.073 MPa/kg, GFRP-R confined concrete is 0.079 MPa/kg and CFRP confined concrete is 0.115 MPa/kg.

The CFRP confined concrete exhibited the highest CSI followed by GFRP-R confined concrete, GFRP-MS confined concrete and unconfined concrete. However, the CFRP confined concrete exhibited the highest CI followed by GFRP-MS confined concrete, GFRP-R confined concrete and unconfined concrete. The GFRP-R confined concrete exhibited CI 0.76 times of CFRP confined concrete, 0.87 times of GFRP-MS confined concrete, and 1.43 times of unconfined concrete. Moreover, GFRP-R confined concrete exhibited CSI of 0.66 times CFRP confined concrete, 1.07 times of GFRP-MS confined concrete and 1.17 times of unconfined concrete. Hence, it is concluded that GFRP-R with high CSI and low CI is a viable option for wide use in the construction industry.

5. Conclusions

This study investigated the influence of the Carbon FRP (CFRP) wrap and locally available low-cost GFRP Matt Strands (GFRP-MS) wrap and GFRP Rowing (GFRP-R) wrap on the axial compressive behavior of FRP confined concrete. The study also examined the influence of two normal strength concrete (NSC) mixes on the axial compressive strength of FRP confined concrete. The experimental program comprised sixteen specimens of 150 mm in diameter and 300 mm in height. A database of 140 FRP wrap confined concrete specimens was established to develop a regression model to predict the FRP confined concrete strength of the tested specimens. The following conclusions are drawn based on the findings presented in this study:

1. The single layer of CFRP confined concrete, GFRP-R confined concrete, and GFRP-MS confined concrete strengths were 1.76, 1.17, and 1.09 times higher, respectively, than the unconfined concrete strengths. The CFRP confined concrete specimens exhibited 1.51 times and 1.62 times higher confined concrete strength, respectively, than the GFRP-R confined concrete and GFRP-MS confined concrete specimens. The CFRP confined concrete specimens exhibited about 2.1 times higher confined concrete strain at the peak axial stress than GFRP-R and GFRP-MS confined concrete specimens. The GFRP-R confined concrete specimens exhibited 1.5 times higher confined concrete strain at peak axial stress than GFRP-MS confined concrete specimens.
2. Mix-B having unconfined concrete strength of 24.3 MPa exhibited about 19.3% larger confined concrete strengths than Mix-A having unconfined concrete strength of 29.3 MPa. However, Mix B showed about 24% lower confined concrete strain at peak axial stress than Mix-A.

3. Locally available low-cost two layers of GFRP-R wrap and four layers of GFRP-MS wrap can give similar confined concrete strength as a single layer of CFRP with 12 times and 6 times lower costs, respectively.
4. A regression model based on FRP confined concrete database comprising experimental results of 140 specimens was proposed to predict the strength enhancement coefficient (k_1). This study proposes k_1 of 3.20 for FRP confined concrete. The experimental and predicted CFRP confined concrete strengths matched well. However, the GFRP-R and GFRP-MS confined concrete strengths were underestimated by about 14.5% and 5%, respectively, by the proposed model.
5. The GFRP-R confined concrete exhibited CI of 0.76 times CFRP confined concrete, 0.87 times of GFRP-MS confined concrete, and 1.43 times of unconfined concrete. Moreover, GFRP-R confined concrete exhibited CSI of 0.66 times CFRP confined concrete, 1.07 times of GFRP-MS confined concrete, and 1.17 times of unconfined concrete.

Locally available low-cost GFRP-R wrap is a viable solution for confined concrete in terms of cost-effectiveness and environmentally friendly benefits.

Author Contributions: Conceptualization, A.U.Q. and T.M.P.; methodology, Q.S.K. and H.A.A.; formal analysis, H.A.A.; data curation, H.A.A.; writing—Q.S.K.; writing—review and editing, Q.S.K. and T.M.P.; supervision, A.U.Q. and Q.S.K. All authors have read and agreed to the published version of the manuscript.

Funding: This research received no external funding.

Institutional Review Board Statement: Not applicable.

Informed Consent Statement: Not applicable.

Data Availability Statement: Some or all of the data may be provided on request.

Acknowledgments: The authors thank Civil Engineering Department, University of Engineering and Technology, Lahore for providing the research facilities to conduct this research study. The authors thank Imporient Chemical (PVT) LTD to provide CFRP wraps and epoxies required in this research study.

Conflicts of Interest: The authors declare no conflict of interest.

References

1. Hadi, M.N.S.; Khan, Q.S.; Sheikh, M.N. Axial and flexural behavior of circular concrete filled FRP tube (CFFT) columns with and without FRP reinforcing bars. *Constr. Build. Mater.* **2016**, *122*, 43–53. [[CrossRef](#)]
2. Khan, Q.S.; Sheikh, M.N.; Hadi, M.N.S. Axial and flexural interactions of GFRP-CFFT columns with and without reinforcing GFRP bars. *J. Compos. Constr.* **2017**, *21*, 3. [[CrossRef](#)]
3. Khan, Q.S.; Sheikh, M.N.; Hadi, M.N.S. Experimental results of circular FRP tube confined concrete (CFFT) and comparison with analytical models. *J. Build. Eng.* **2020**, *29*, 101157. [[CrossRef](#)]
4. Khan, Q.S.; Sheikh, M.N.; Hadi, M.N.S. Axial compressive behavior of circular CFFT: Experimental database and design-oriented model. *Steel Compos. Struct. Int. J.* **2016**, *21*, 921–947. [[CrossRef](#)]
5. Raza, S.; Khan, M.K.I.; Menegon, S.I.; Tsang, H.; Wilson, J.L. Strengthening and repair of reinforced concrete columns by jacketing: State of the Art. *Sustainability* **2019**, *11*, 3208. [[CrossRef](#)]
6. Sánchez, M.; Faria, P.; Ferrara, L.; Horszczaruk, E.; Jonkers, H.M.; Kwiecień, A.; Mosa, J.; Peled, A.; Pereira, A.S.; Snoeck, D.; et al. External treatments for the preventive repair of existing constructions: A review. *Constr. Build. Mater.* **2018**, *193*, 435–452. [[CrossRef](#)]
7. Hadi, M.N.S.; Algburi, A.H.M.; Neaz, M.S.; Carrigan, A.T. Axial and flexural behavior of circular reinforced concrete columns strengthened with reactive powder concrete jacket and fiber reinforced polymer wrapping. *Constr. Build. Mater.* **2018**, *172*, 717–727. [[CrossRef](#)]
8. Yazici, V.; Hadi, M. Axial Load-Bending Moment Diagrams of carbon FRP wrapped hollow core reinforced concrete columns. *J. Compos. Constr.* **2009**, *13*, 262–268. [[CrossRef](#)]
9. De Lorenzis, L.; Tepfers, R. Comparative study of models on confinement of concrete cylinders with Fiber-Reinforced Polymer composites. *J. Compos. Constr.* **2003**, *7*, 219–237. [[CrossRef](#)]
10. Pham, T.; Hadi, M. Stress prediction model for FRP confined rectangular concrete columns with rounded corners. *J. Compos. Constr.* **2014**, *18*, 04013019. [[CrossRef](#)]

11. Attari, N.; Amziane, S.; Chemrouk, M. Flexural strengthening of concrete beams using CFRP, GFRP and hybrid FRP sheets. *Constr. Build. Mater.* **2012**, *37*, 746–757. [CrossRef]
12. Khan, Q.S.; Sheikh, M.N.; Hadi, M.N.S. Concrete Filled Carbon FRP Tube (CFRP-CFFT) columns with and without CFRP reinforcing bars: Axial-flexural interactions. *Compos. Part B Eng.* **2018**, *133*, 42–52. [CrossRef]
13. Khan, Q.S.; Sheikh, M.N.; Hadi, M.N.S. Experimental and analytical investigations of CFFT columns with and without FRP bars under concentric compression. *Steel Compos. Struct. Int. J.* **2019**, *30*, 591–601.
14. Rizkalla, S.; Hasan, T.; Nahla, H. Design recommendations for the use of FRP for reinforcement and strengthening of concrete structures. *Prog. Struct. Eng. Mater.* **2003**, *5*, 16–28. [CrossRef]
15. Khan, Q.S.; Sheikh, M.N.; Hadi, M.N.S. Predicting strength and strain enhancement ratios of circular fiber-reinforced polymer tube confined concrete under axial compression using artificial neural networks. *Adv. Struct. Eng.* **2019**, *22*, 1426–1443. [CrossRef]
16. Khan, Q.S.; Sheikh, M.N.; Hadi, M.N.S. Tensile testing of carbon FRP (CFRP) and Glass FRP (GFRP) bars: An experimental study. *ASTM J. Test. Eval.* **2021**, *49*, 20180660. [CrossRef]
17. Ozbakkaloglu, T.; Lim, J.C. Axial compressive behavior of FRP-confined concrete: Experimental test database and a new design-oriented model. *Compos. Part B Eng.* **2013**, *55*, 607–634. [CrossRef]
18. Siddhartha, M.; Andrew, H.; Amir, F. Influence of concrete strength on confinement effectiveness of fiber-reinforced polymer circular jackets. *ACI Struct. J.* **2005**, *102*, 383.
19. Cui, C.; Sheikh, S.A. Experimental study of normal-and high-strength concrete confined with fiber-reinforced polymers. *J. Compos. Constr.* **2010**, *14*, 553–561. [CrossRef]
20. Ozbakkaloglu, T.; Akin, E. Behavior of FRP-confined normal-and high-strength concrete under cyclic axial compression. *J. Compos. Constr.* **2011**, *16*, 451–463. [CrossRef]
21. Vincent, T.; Ozbakkaloglu, T. Influence of fiber orientation and specimen end condition on axial compressive behavior of FRP-confined concrete. *Constr. Build. Mater.* **2013**, *47*, 814–826. [CrossRef]
22. Vincent, T.; Ozbakkaloglu, T. Compressive behavior of prestressed high-strength concrete-filled Aramid FRP tube columns: Experimental observations. *J. Compos. Constr.* **2015**, *19*, 04015003. [CrossRef]
23. Aire, C.; Gettu, R.; Casas, J.R.; Marques, S.; Marques, D. Estudio experimental y modelo teórico del hormigón confinado lateralmente con polímeros reforzados con fibras (FRP). *Mater. Constr.* **2010**, *60*, 19–31. [CrossRef]
24. Chikh, N.; Gahmous, M.; Benzaid, R. Structural performance of high strength concrete columns confined with CFRP sheets. In Proceedings of the World Congress on Engineering, London, UK, 4–6 July 2012.
25. Harajli, M.H. Axial stress—Strain relationship for FRP confined circular and rectangular concrete columns. *Cem. Concr. Compos.* **2006**, *28*, 938–948. [CrossRef]
26. Pham, T.M.; Hadi, M.N.S. Confinement model for FRP confined normal- and high-strength concrete circular columns. *Constr. Build. Mater.* **2014**, *69*, 83–90. [CrossRef]
27. Lam, L.; Teng, J.G. Design-oriented stress—Strain model for FRP-confined concrete. *Constr. Build. Mater.* **2003**, *17*, 471–489. [CrossRef]
28. Berthet, J.F.; Ferrier, E.; Hamelin, P. Compressive behavior of concrete externally confined by composite jackets. *Constr. Build. Mater.* **2006**, *20*, 338–347. [CrossRef]
29. Wu, G.; Lü, Z.T.; Wu, Z.S. Strength and ductility of concrete cylinders confined with FRP composites. *Constr. Build. Mater.* **2006**, *20*, 134–148. [CrossRef]
30. Teng, J.G.; Jiang, T.; Lam, L.; Luo, Y.Z. Refinement of a design-oriented stress—Strain model for FRP-confined concrete. *J. Compos. Constr.* **2009**, *13*, 269–278. [CrossRef]
31. Wei, Y.; Wu, Y. Unified stress—Strain model of concrete for FRP-confined columns. *Constr. Build. Mater.* **2012**, *26*, 381–392. [CrossRef]
32. Fardis, M.N.; Khalili, H.H. FRP-encased concrete as a structural material. *Mag. Concr. Res.* **1982**, *34*, 191–202. [CrossRef]
33. Ahmad, S.M.; Khaloo, A.R.; Irshad, A. Behavior of concrete spirally confined by fiberglass filaments. *Mag. Concr. Res.* **1991**, *43*, 143–148. [CrossRef]
34. Howie, I.; Karbhari, V.M. Effect of Tow sheet composite wrap architecture on strengthening of concrete due to confinement: I—Experimental Studies. *J. Reinf. Plast. Compos.* **1995**, *14*, 1008–1030. [CrossRef]
35. Owen, L.M. *Stress—Strain Behavior of Concrete Confined by Carbon Fiber Jacketing*; University of Washington: Seattle, WA, USA, 1998.
36. Matthys, S.; Toutanji, H.; Taerawe, L. Stress—Strain Behavior of Large-Scale Circular Columns Confined with FRP Composites. *J. Struct. Eng.* **2006**, *132*, 123–133. [CrossRef]
37. Jiang, T.; Teng, J.G. Analysis-oriented stress—Strain models for FRP—Confined concrete. *Eng. Struct.* **2007**, *29*, 2968–2986. [CrossRef]
38. *ASTM C192/C192M-14 (ASTM 2014)*; Standard Practice for Making and Curing Concrete Test Specimens in the Laboratory. ASTM International: West Conshohocken, PA, USA, 2014.
39. Imporient Chemicals. Imporient Chemicals Lahore, Pakistan. 2020. Available online: <https://imporientgroup.com> (accessed on 21 January 2022).
40. *ASTM D3039-17 (ASTM 2017)*; International Standard Test Method for Tensile Properties of Polymer Matrix Composite Materials. ASTM International: West Conshohocken, PA, USA, 2017.

41. ASTM C39-18 (ASTM 2018); International Standard Test Method for Compressive Strength of Cylindrical Concrete Specimens. ASTM International: West Conshohocken, PA, USA, 2018.
42. Richart, F.E.; Anton, B.; Lenoir, B.R. *A study of the Failure of Concrete under Combined Compressive Stresses*; University of Illinois: Champaign, IL, USA, 1928.
43. Lea, G.; Elie, A.; George, S.; Helmi, K.; Mounir, M. Concrete columns wrapped with Hemp fiber reinforced polymer—An Experimental Study. *Procedia Eng.* **2017**, *200*, 440–447.
44. Vincent, T.; Ozbakkaloglu, T. Influence of concrete strength and confinement method on axial compressive behavior of FRP confined high- and ultra high-strength concrete. *Compos. Part B Eng.* **2013**, *50*, 413–428. [[CrossRef](#)]
45. Tara, S.; Ashim, P. Confining concrete with sisal and jute FRP as alternatives for CFRP and GFRP. *Int. J. Sustain. Built Environ.* **2015**, *4*, 248–264.
46. Jalal, M.; Ramezani-pour, A.A. Strength enhancement modeling of concrete cylinders confined with CFRP composites using artificial neural networks. *Compos. Part B Eng.* **2012**, *43*, 2990–3000. [[CrossRef](#)]
47. Akogbe, K.; Meng, L.; Zhi-Min, W. Size effect of axial compressive strength of CFRP confined concrete cylinders. *Int. J. Concr. Struct. Mater.* **2011**, *5*, 49–55. [[CrossRef](#)]
48. Dai, J.; Yu-Lei, B.; Teng, J.G. Behavior and modeling of concrete confined with FRP composites of large deformability. *J. Compos. Constr.* **2011**, *15*, 963–973. [[CrossRef](#)]
49. Eid, R.; Roy, N.; Paultre, P. Normal-and high-strength concrete circular elements wrapped with FRP composites. *J. Compos. Constr.* **2009**, *13*, 113–124. [[CrossRef](#)]
50. Almusallam, T.H. Behavior of normal and high-strength concrete cylinders confined with E-glass/epoxy composite laminates. *Compos. Part B Eng.* **2007**, *38*, 629–639. [[CrossRef](#)]
51. Valdmanis, V.; De Lorenzis, L.; Theodoros, R.; Tepfers, R. Behavior and capacity of CFRP-confined concrete cylinders subjected to monotonic and cyclic axial compressive load. *Struct. Concr. Lond. Thomas Telford Ltd.* **2007**, *8*, 187.
52. Wu, Y.; Wang, L. Unified strength model for square and circular concrete columns confined by external jacket. *J. Struct. Eng.* **2009**, *135*, 253–261. [[CrossRef](#)]
53. Picher, F. Confinement de Cylinders en Béton Par Des Composites Carbone-éPoxy Unidirectionnels. Master's Thesis, University of Sherbrooke, Sherbrooke, QC, Canada, 1995.
54. Tamuzs, V.; Tepfers, R.; Chi-Sang, Y.; Rousakis, T.; Repelis, I.; Skruls, V.; Vilks, U. Behavior of concrete cylinders confined by carbon-composite tapes and prestressed yarns 1. Experimental data. *Mech. Compos. Mater.* **2006**, *42*, 13–32. [[CrossRef](#)]
55. Lam, L.; Teng, J.G.; Cheung, C.H.; Xiao, Y. FRP-confined concrete under axial cyclic compression. *Cem. Concr. Compos.* **2006**, *28*, 949–958. [[CrossRef](#)]
56. Campione, G. Influence of FRP wrapping techniques on the compressive behavior of concrete prisms. *Cem. Concr. Compos.* **2006**, *28*, 497–505. [[CrossRef](#)]
57. Lam, L.; Teng, J.G. Ultimate condition of fiber reinforced polymer-confined concrete. *J. Compos. Constr.* **2004**, *8*, 539–548. [[CrossRef](#)]
58. Theriault, M.; Neale, K.W.; Claude, S. Fiber-reinforced polymer-confined circular concrete columns: Investigation of size and slenderness effects. *J. Compos. Constr.* **2004**, *8*, 323–331. [[CrossRef](#)]
59. Harries, K.A.; Carey, S.A. Shape and “gap” effects on the behavior of variably confined concrete. *Cem. Concr. Res.* **2003**, *33*, 881–890. [[CrossRef](#)]
60. Ibrahim, S.A.E.M.; Luiz, C.A.V.; Lidia, S.C.D. Strength of short concrete columns confined with CFRP sheets. *Mater. Struct.* **2002**, *35*, 50–58.
61. Rousakis, T.; Tepfers, R. Experimental investigation of concrete cylinders confined by carbon FRP sheets, under monotonic and cyclic axial compressive load. *Res. Rep.* **2001**, 1–10.
62. Shahawy, M.; Mirmiran, A.; Beitelman, T. Tests and modeling of carbon-wrapped concrete columns. *Compos. Part B Eng.* **2000**, *31*, 471–480. [[CrossRef](#)]
63. Xiao, Y.; Wu, H. Compressive behavior of concrete confined by carbon fiber composite jackets. *J. Mater. Civ. Eng.* **2000**, *12*, 139–146. [[CrossRef](#)]
64. Karbhari, V.M.; Gao, Y. Composite jacketed concrete under uniaxial compression—Verification of simple design equations. *J. Mater. Civ. Eng.* **1997**, *9*, 185–193. [[CrossRef](#)]
65. Wu, Y.; Zhou, Y. Unified strength model based on Hoek-Brown failure criterion for circular and square concrete columns confined by FRP. *J. Compos. Constr.* **2010**, *14*, 175–184. [[CrossRef](#)]
66. Pour, A.F.; Ozbakkaloglu, T.; Vincent, T. Simplified design-oriented axial stress-strain model for FRP-confined normal- and high-strength concrete. *Eng. Struct.* **2018**, *175*, 501–516. [[CrossRef](#)]
67. Park, S.; Wu, S.; Lu, Z.; Pyo, S. The role of supplementary cementitious materials (SCMs) in ultra-high performance concrete (UHPC): A review. *Materials* **2021**, *14*, 1472. [[CrossRef](#)] [[PubMed](#)]
68. Mara, V.; Hoghani, R.; Harryson, P. Bridge decks of fiber reinforced polymer (FRP): A sustainable solution. *Constr. Build. Mater.* **2014**, *50*, 190–199. [[CrossRef](#)]
69. Jiang, C.; Wu, Y. Axial strength of eccentrically loaded FRP confined short concrete columns. *Polymers* **2020**, *12*, 1261. [[CrossRef](#)]